

Spread and erase - How electron hydrodynamics can eliminate the Landauer-Sharvin resistance

Ady Stern,¹ Thomas Scaffidi,² Oren Reuven,¹ Chandan Kumar,¹ John Birkbeck,¹ and Shahal Ilani¹

¹*Department of Condensed Matter Physics, Weizmann Institute of Science, Rehovot 76100, Israel*

²*Department of Physics, University of Toronto, 60 St. George Street, Toronto, Ontario, M5S 1A7, Canada*

It has long been realized that even a perfectly clean electronic system harbors a Landauer-Sharvin resistance, inversely proportional to the number of its conduction channels. This resistance is usually associated with voltage drops on the system's contacts to an external circuit. Recent theories have shown that hydrodynamic effects can reduce this resistance, raising the question of the lower bound of resistance of hydrodynamic electrons. Here we show that by a proper choice of device geometry, it is possible to spread the Landauer-Sharvin resistance throughout the bulk of the system, allowing its complete elimination by electron hydrodynamics. We trace the effect to the dynamics of electrons flowing in channels that terminate within the sample. For ballistic systems this termination leads to back-reflection of the electrons and creates resistance. Hydrodynamically, the scattering of these electrons off other electrons allows them to transfer to transmitted channels and avoid the resistance. Counter-intuitively, we find that in contrast to the ohmic regime, for hydrodynamic electrons the resistance of a device with a given width can decrease with its length, suggesting that a long enough device may have an arbitrarily small total resistance.

Introduction The resistivity of an electronic system to the flow of current is a fundamental quantity in condensed matter physics. Frequently, its minimization is to be desired. The Drude model, dating back to 1900, suggests that the resistivity originates mostly from momentum loss to impurities. However, it was realized that even in the ballistic limit, in which impurities and phonons are absent, the interface between the electronic system and the metallic contacts to which it is coupled carries another fundamental source of resistance - the Landauer-Sharvin resistance[1–4]. As stated by Landauer's formula, this resistance is inversely proportional to the number of quantum mechanical channels that are transmitted through the system.

More recently, motivated by experiments in two-dimensional materials, another regime of transport was discovered in which electrons behave like a viscous fluid due to strong momentum-conserving electron-electron scattering. In this regime, Ohm's law is supplanted by the much richer Navier-Stokes equation, which leads to a flurry of interesting effects[5–48]. Somewhat counter-intuitively, it was also shown that this hydrodynamic regime of transport can have a resistance which is even lower than the ballistic one, and hence dubbed "super-ballistic"[29, 30]. Furthermore, conditions in which field-free current flow may locally exist were suggested[40].

In this work, using a combination of Landauer and Boltzmann analyses we demonstrate a mechanism by which electron hydrodynamics can eliminate the Landauer-Sharvin resistance, and find the minimal value that this resistance may attain. Our study is semi-classical and focuses on two dimensional systems. We describe an electronic system in terms of its conduction channels, and show that when the number of channels varies along the direction of the current flow, the Landauer-Sharvin resistance detaches from the contacts

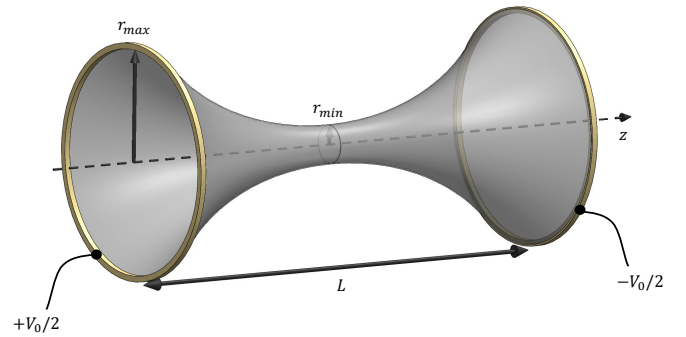


FIG. 1. The wormhole geometry is a two dimensional azimuthally-symmetric electronic system embedded in three dimensional space, described by the equation $r = r(z)$, where the radius is maximal (r_{max}) at the interface to the contacts and minimal (r_{min}) at the center. A current I is driven from negative to positive z , and the potentials at the two contacts are $V(\mp L/2) = \pm \frac{V_0}{2}$.

and spreads over the bulk of the electronic system. When the length scale of this spreading is larger than the electron-electron scattering mean free path, ℓ_{ee} , the resistance is dramatically suppressed.

Microscopically, this suppression results from the scattering of electrons whose channels are being terminated due to a narrowing of the electronic system's cross-section or a decrease of its carrier density. In a ballistic system, these electrons are reflected back and do not contribute to the current, thereby generating Landauer-Sharvin resistance in the sample's bulk. In contrast, in the hydrodynamic regime electron-electron scattering transfers these electrons into transmitted channels, thus avoiding their reflection and the corresponding resistance.

Equipped with this analysis, we can ask the question of the minimal resistance of hydrodynamic elec-

trons flowing through a constriction. In the ballistic case, for a sample of length L and a minimal cross section $2\pi r_{min}$, the Landauer-Sharvin resistance is given by $\frac{h}{2e^2 k_F r_{min}}$ (k_F is the Fermi momentum, and we consider a single spin species). In the hydrodynamic case, previous works[29, 30, 40] reported a reduction of the Landauer resistance by a factor of ℓ_{ee}/r_{min} due to electron hydrodynamics. As we show below, this resistance may be further reduced by an additional factor of r_{min}/L if the constriction's width varies over a scale $L \gg r_{min}$. Counter-intuitively, in contrast to the familiar ohmic regime, in which resistance increases with L , the resistance in the hydrodynamic regime decreases with L . This implies that a system with a given r_{min} and a large enough L may have an arbitrarily small total resistance.

Wormhole geometry In order to study the resistance of hydrodynamic electrons in a generic expanding geometry while avoiding boundary effects, we use a ‘‘wormhole’’ geometry (Fig. (1)). This geometry is a two-dimensional surface of revolution embedded in three dimensions, with azimuthal symmetry (toward the end of the paper we consider also a Corbino disk and a bar with varying electronic density). In cylindrical coordinates, the wormhole is defined by $r = r(z)$, with its minimum radius, r_{min} , occurring at $z = 0$, and maximum radius, r_{max} , occurring at the contacts positioned at $z = \pm L/2$. For simplicity we assume $r(z) = r(-z)$. A current I driven through the wormhole in the z -direction leads to a potential $V(z = \mp L/2) = \pm \frac{V_0}{2}$ at its contacts. On the manifold, we define a Cartesian local coordinate system tangent to the manifold, in which y is the azimuthal direction, and x is the direction along the manifold. For brevity, we set $\hbar = e = 1$.

Boltzmann description Time-independent transport in a wormhole geometry may be described by a Boltzmann equation. In the absence of a driving force, the equation reads (see appendix for derivation):

$$\cos\theta\partial_z f - \frac{r'}{r}\sin\theta\partial_\theta f = \sqrt{1+r'^2}I[f] \quad (1)$$

where $f(\mathbf{r}, \mathbf{p})$ is the deviation of the number of electrons in a position \mathbf{r} with momentum \mathbf{p} from its equilibrium value, θ is the angle of the momentum with respect to the x -direction, $r' \equiv dr/dz$, and $I[f]$ is the scattering integral, elaborated below.

It is common to substitute the ansatz

$$f(\mathbf{p}, \mathbf{r}) = \delta(\epsilon_F - \epsilon(\mathbf{p}))h(\mathbf{p}, \mathbf{r}) \quad (2)$$

in (1), and integrate both sides over the magnitude of the momentum $\int \frac{pdp}{4\pi^2}$, with $p = |\mathbf{p}|$. This integration fixes $|\mathbf{p}| = p_F$ such that h becomes a function of \mathbf{r} and θ , which describes the non-equilibrium angular shape of the Fermi surface. The integration replaces the δ -function in (2) by a density of states at the Fermi energy and angle θ , $\nu(E_F, \theta) = \nu_F/2\pi$ (here ν_F is the density of states

at the Fermi energy). The Boltzmann equation becomes an equation for $\nu_F h(\theta, \mathbf{r})/2\pi$. The azimuthal symmetry reduces the dependence on \mathbf{r} to a dependence on z only.

Landauer description In the Landauer picture, the system is composed of $2j_{max} + 1$ channels, enumerated by their angular momentum $j = -j_{max}..0..j_{max}$, with $j_{max} = k_F r_{max}$. The angular momentum $j = p_y(z)r(z)$, with p_y the momentum in the azimuthal direction. Each channel is characterized by transmission and reflection probabilities T_j, R_j satisfying $T_j + R_j = 1$. We assume $r(z)$ to vary slowly on the scale of the Fermi wavelength, such that in the absence of interactions, channels with $|j| < k_F r_{min}$ are fully transmitted, and all other channels are fully reflected, with the reflection taking place at the classical turning point $r(z) = |j|/k_F$. The current flowing through the wormhole is $I = \frac{k_F r_{min}}{\pi} V_0$, leading to the dimensionless Landauer-Sharvin resistance being $R_{ballistic} = \pi/k_F r_{min}$.

‘‘Landauerizing’’ Boltzmann We now reformulate the Boltzmann equation to elucidate its relation to the Landauer picture. To that end, we express the shape of the Fermi surface in terms of a different set of variables - the channel angular momentum j , the direction of motion, right (R) or left (L), and the position, z . In the semi-classical Boltzmann equation the angular momentum is a real number, and it is quantized to an integer in Landauer's quantum mechanical analysis. Here, we think about it semi-classically.

Two steps are needed in order to transform the Boltzmann equation from an equation for $h(\theta, z)$ to an equation for the occupation in terms of j, z and direction of motion, which we will denote by $h_{R,L}^j(z)$. First, we need to change the variables in Eq. (1). Second, the integral $\int \frac{pdp}{4\pi^2}$ should be replaced by an integral over the x -component of the momentum, namely $p_F \int \frac{dp_x}{2\pi}$, where the limits are given by $p_x = 0$ and $p_x = \pm\infty$, for R,L respectively. The δ -function in (2) is then replaced by a density of states at the Fermi level at a fixed $j = p_y r(z)$,

$$\nu^j = \frac{\nu_F}{\sqrt{1 - \left(\frac{j}{k_F r(z)}\right)^2}} \quad (3)$$

with $|j| \leq k_F r(z)$. This density of states is inversely proportional to the x -component of the velocity, as familiar from Landauer's analysis. The details of the transformation are given in the Appendix, but the outcome is quite expected from the conservation of angular momentum:

$$\pm \nu_F \partial_z h_{R,L}^j(z) = \sqrt{1+r'^2} \tilde{I}[h_{R,L}^j(z)] \quad (4)$$

where the \pm refers to right and left moving electrons, and \tilde{I} is the scattering term expressed as a functional of $h_{R,L}^j(z)$, derived below.

The electronic density $\rho(z)$, current density $J_x(z)$ and

potential $V(z)$ are,

$$\begin{aligned}\rho(z) &= \int \frac{d\mathbf{p}}{4\pi^2} f(\mathbf{p}, z) = \frac{1}{2\pi k_F r(z)} \int dj \nu^j(z) [h_R^j + h_L^j] \\ J_x(z) &= \int \frac{d\mathbf{p}}{4\pi^2} \frac{p_x}{m} f(\mathbf{p}, z) = \frac{1}{4\pi^2 r(z)} \int dj [h_R^j - h_L^j] \\ V(z) &= \rho(z)/\nu_F\end{aligned}\quad (5)$$

Ballistic regime. In the absence of collisions ($\tilde{I} = 0$), Eq. (4) states that there is no inter-channel scattering along the wormhole, which is a consequence of angular momentum conservation. As for intra-channel back-scattering, two situations may exist: fully transmitted channels are those for which $j < k_F r_{min}$. For these channels, each of the two non-equilibrium occupations $h_{R,L}^j(z)$ is determined by the contact from which it emanates, and is independent of z . In contrast, if there is a point z_0 for which $j = k_F r(z_0)$, at this point the channel is fully reflected. Since the momentum has no x -component at z_0 , the occupations of the right and left movers are the same, i.e., $h_R^{j=\pm k_F r(z_0)}(z_0) = h_L^{j=\pm k_F r(z_0)}(z_0)$. The value of these functions remains the same on one side of z_0 where the channel exists, with the value determined by the contact from which the channel emanates and to which it is back-reflected. Both occupations vanish at the other side of z_0 , in which the channel does not exist. Figure (2a,b) presents $h_R^j \mp h_L^j$ for a particular example of a ballistic wormhole, showing the non-equilibrium channel-dependent contributions to the local potential and current density.

Each contact feeds into the wormhole all channels below its potential, $\pm V_0/2$ for the left and right contacts respectively, thus specifying the boundary conditions. By Landauer's formula, $V_0 = \pi I/k_F r_{min}$. With these boundary conditions, we can solve for $h_{R,L}^j(z)$ and use the solution to calculate the potential as a function of z . We find the potential to be,

$$\begin{aligned}V_{ballistic}(z) &= -\text{sgn}(z) \frac{V_0}{\pi} \int_{k_F r_{min}}^{k_F r(z)} \frac{dj}{\sqrt{(k_F r(z))^2 - j^2}} \\ &= -\text{sgn}z \frac{V_0}{2} \left[1 - \frac{2}{\pi} \arcsin \frac{r_{min}}{r(z)} \right]\end{aligned}\quad (6)$$

Interestingly, although there are no collisions, we see that there is a potential drop, and thus resistance, in the bulk of the wormhole. Eq. (6) shows that the potential close to the edges of the wormhole ($z = \pm L/2$) is smaller than that in the contacts themselves by $\frac{V_0}{\pi} \arcsin \frac{r_{min}}{r_{max}}$. This difference is the Landauer-Sharvin contact resistance. In the limit $r_{max} \gg r_{min}$ this contact resistance becomes negligible, and practically all the Landauer-Sharvin resistance drops in the bulk. From Eq. (6) we see that voltage drops in the bulk when the upper limit of the integral varies with z . This shows that the bulk Landauer-Sharvin resistance appears whenever the number of conduction channels varies in the bulk. As we

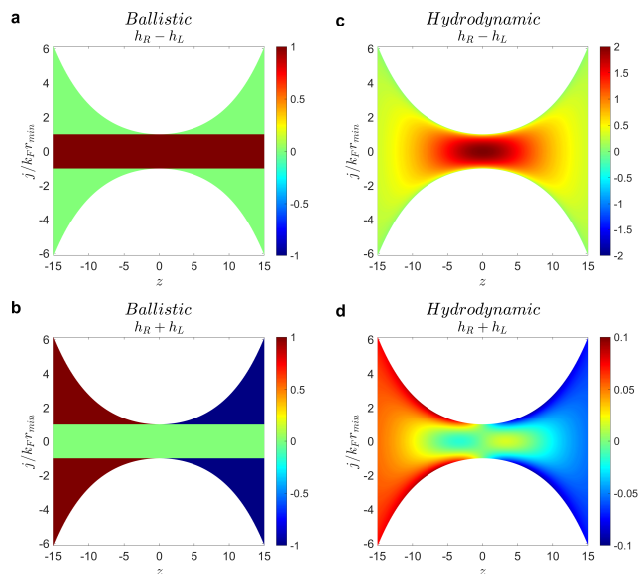


FIG. 2. Non-equilibrium distribution functions $h_R - h_L$ and $h_R + h_L$ for ballistic (a,b) and hydrodynamic (c,d) cases. These distribution functions contribute to the current density and voltage respectively (see Eq. (5)). They are plotted for the wormhole defined in (11) with $a/r_0 = 6$, as a function of the spatial coordinate z , and the normalized channel index, $j/k_F r_{min}$. In panels (c,d) $\ell_{ee}/r_0 = 0.3$. Green color corresponds to zero population, while white reflects states above the Fermi energy.

show below, electron-electron scattering can dramatically suppress the bulk potential drop, allowing the system to conduct much better than the fundamental Landauer-Sharvin limit.

Electron-electron scattering and the hydrodynamic regime. We now turn to consider the effect of momentum conserving electron-electron interactions on the wormhole resistance. Within the relaxation time approximation, and taking conservation laws into account [11, 49], we have

$$I[f(\mathbf{p}, \mathbf{r})] = -\frac{1}{\ell_{ee}} \left[f - \frac{\delta(\epsilon_F - \epsilon(\mathbf{p}))}{\nu_F} (\rho(\mathbf{r}) + \frac{2J_x(\mathbf{r}) \cos \theta}{\nu_F}) \right]\quad (7)$$

The second term on the right hand side guarantees charge conservation, while the third term guarantees momentum conservation. We obtain $\tilde{I}[h^j]$ by using the same ansatz we used before,

$$\begin{aligned}\tilde{I}[h_{R,L}^j(z)] &= \\ &= -\frac{\nu^j}{\ell_{ee}} \left[h_{R,L}^j(z) - \frac{\rho(z)}{\nu_F} \mp \frac{4\pi J_x(z)}{k_F} \sqrt{1 - \left(\frac{j}{k_F r(z)} \right)^2} \right]\end{aligned}\quad (8)$$

The ν^j/ℓ_{ee} factor makes the mean free path j -dependent and shortens it from ℓ_{ee} to $\ell_{ee} \sqrt{1 - \left(\frac{j}{k_F r(z)} \right)^2}$. This

may be traced back to the observation that for larger $j/r(z)$, p_x is smaller and a shorter distance is traversed in the z -direction between two scattering events. In particular, the scattering length vanishes when the channel is about to be terminated, opening a way for the electrons to avoid back-scattering by being scattered to a transmitted channel. Furthermore, in contrast to the case of impurity scattering, in which in Eq. (8) ℓ_{ee} is replaced by a momentum-relaxing mean free path and the third term is absent, here the presence of the third term allows for a Galilean boost of the Fermi surface $h_{R,L}^j(z) = \pm \frac{4\pi J_x(z)}{k_F} \sqrt{1 - (j/k_F r(z))^2}$ to be carried out without developing a resistance.

We find the solution to a leading order in ℓ_{ee} (the calculation is given in the Appendix),

$$\begin{aligned} h_{R,L}^j(z) = & \pm \frac{2I}{k_F r(z)} \sqrt{1 - \left(\frac{j}{k_F r(z)}\right)^2} \\ & + \frac{2I\ell_{ee} \sin \xi(z)}{k_F r^2(z)} \left[1 - 2\left(\frac{j}{k_F r(z)}\right)^2\right] \\ & - \int_0^z \frac{I\ell_{ee}}{k_F r^2(z')} \cos \xi(z') \frac{d\xi}{dz'}(z') dz' \quad (9) \end{aligned}$$

where $\xi(z)$ is the local angle between z -axis and the manifold, and consequently $r(z)' = \tan \xi(z)$. This solution is valid in the bulk, away from the contacts. We comment on the role of the contacts below, with details in the Appendix.

The first term in Eq. (9) is a rigidly shifted Fermi surface, which is the solution expected for $r' = 0$ far away from the contacts, after all deformations of the Fermi surface are suppressed by the scattering term. The second and third terms are smaller than the first by a factor of $\ell_{ee}/r(z)$, and originate from the breaking of Galilean invariance. The second term makes the shifted Fermi surface acquire an elongated shape, with more electrons in the head-on direction (small j), and less in the $j \approx k_F r(z)$ channels. The third term is independent of j . It carries an electronic density, and thus leads to a potential drop and a resistivity. Note that while the second term exists when $\sin \xi \neq 0$, the third term with its voltage drop requires $\frac{d \sin \xi}{dz} \neq 0$. Stated differently, in contrast to ballistic electrons for which local resistance appears when the number of conduction channels varies with z , i.e., when $r' \neq 0$, for hydrodynamic electrons resistance is generated only when this function has a non-zero curvature, $r'' \neq 0$.

The potential originating from the third term of Eq. (9) may be written also as an integral over ξ :

$$V_{\text{hydro}}(z) = I \int_0^{\xi(z)} \frac{\ell_{ee}}{4\pi k_F r^2(\xi)} \cos \xi d\xi \quad (10)$$

The hydrodynamic resistance scale may be estimated from Eq. (10). The r^2 in the denominator suggests that the wormhole resistance is characterized by a

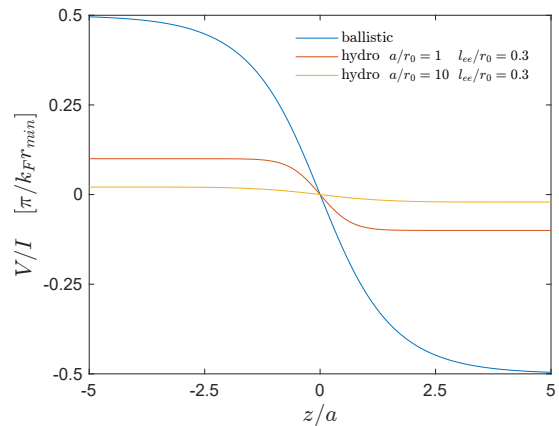


FIG. 3. The potential along the wormhole defined in (11), divided by the current, V/I , in units of the Landauer-Sharvin resistance, plotted for a ballistic flow ($\ell_{ee} = \infty$) and hydrodynamic flows ($\ell_{ee}/r_{min} = 0.3$) with varying values of a/r_0 (see legend).

”super-ballistic” scale [29, 30, 40, 48], $\frac{2\pi\ell_{ee}}{k_F r_{min}^2}$, smaller by $2\ell_{ee}/r_{min}$ than the ballistic Landauer-Sharvin resistance. However, Eq. (10) opens the way for a much smaller scale, $\frac{\ell_{ee}}{4\pi k_F r_{min}^2} \sin \xi_0$, where ξ_0 is the angle at which r becomes much larger than r_{min} . If r grows slowly, $\sin \xi_0$ may be much smaller than one, with the resistance becoming much smaller than the super-ballistic scale. Consequently, for a fixed $r_{max} \gg r_{min}$ the resistance generally decreases with increasing L , opposite to the familiar ohmic dependence.

To illustrate the two hydrodynamic scales, consider an example in which

$$r(z) = r_0 \cosh z/a \quad (11)$$

In this wormhole $r_{min} = r_0$ and $r_{max} \gg r_{min}$ for $L \gg a$. Under the latter condition, the contribution to the resistance decays fast with $|z| \gg a$, and we can take $L \rightarrow \infty$. Then, using Eq. (10) we find

$$R_{\text{cosh}} = \frac{\ell_{ee}}{2\pi k_F} \left[\frac{1}{r_0^2 - a^2} - \frac{a^2 \operatorname{arctanh} \frac{\sqrt{r_0^2 - a^2}}{r_0}}{r_0 (r_0^2 - a^2)^{3/2}} \right] \quad (12)$$

In the limit $a \rightarrow 0$ the resistance tends to $\frac{\ell_{ee}}{2\pi k_F r_0^2}$, but when $a \gg r_0$ the resistance decreases to become of order $\frac{\ell_{ee}}{4\pi k_F r_0 a}$. As can be seen in Eq. (10), most of the resistance originates from the product of the minimum radius r_{min} and the change in angle $\Delta \xi$ over which the radius becomes significantly larger than r_0 . When $a \gg r_0$ the change in angle is $\Delta \xi \sim r_0/a$ and hence the decrease in resistance. Fig. (2c,d) show the calculated $h_L - h_R$ and $h_L + h_R$ for hydrodynamic flow in the wormhole in Eq. (11). These quantities contribute to the current density and potential, respectively (Eq. (5)). Fig. (3) shows potential drop in this wormhole as a function of z , in

the ballistic case and in the hydrodynamic cases for two values of a/r_0 . The hydrodynamic suppression of the resistance with increasing a is clearly visible.

Our analysis reveals the reason for this suppression of the resistance: the source of a potential drop is a reflection of electrons. In the ballistic regime the contact sends into the sample electrons in channels for which j is too large to be transmitted. Those electrons are reflected, and their reflection creates a voltage drop (Eq. (6)). In contrast, in the hydrodynamic regime electrons of high j are scattered to channels of smaller j , such that they largely end up being transmitted, without generating a potential drop.

Eqs. (10) and (11) may be used also to show that the bulk resistance of a Corbino disk vanishes, as a consequence of the lack of variation of ξ . With the limitation of z to a proper range, and with the limit $a \rightarrow 0$, Eq. (11) may be used to describe a Corbino disk. The resulting bulk resistance vanishes in that limit. Indeed, in a Corbino disk the number of channels grows linearly with the radial coordinate, such that its second derivative vanishes, and so does the hydrodynamic resistance. It should be stressed, however, that this vanishing bulk resistance is in series with a contact resistance which in this case is $\pi/(2k_F r_{min})$, where r_{min} is the inner radius of the disk.

Finally, although the wormhole is illuminating theoretically, it is a rather exotic geometry for real-life transistor devices. The latter typically have a simple long rectangular bar geometry, in which the density varies along the x -axis such that it is maximal near the contacts. In a bar geometry, previous work (e.g. [27]) has focused on a viscous contribution arising from the no-slip boundary condition, but in this case we neglect this contribution by assuming specular boundary scattering, or the use of a wide bar. By carrying out an analysis similar to that carried out for the wormhole (see the Supplemental Material), we find the resistance to be

$$R_{bar} = \int_{-\infty}^{\infty} dx \frac{(k'_F \ell_{ee})'}{2k_F^2 r}. \quad (13)$$

Here we account also for the possibility that ℓ_{ee} varies with the variation of k_F . Assuming that the change in k_F is much larger than its minimal value, we can estimate $R \sim \ell_{ee}/k_F r a$, where a is the scale over which k_F and ℓ_{ee} become much larger than their minimal value.

In summary, we showed here that when the Landauer-Sharvin resistance of an electronic system is spread into the bulk of a system, rather than being localized at the interface with the contacts, electron-electron scattering may significantly reduce this resistance, in principle all the way down to zero.

We would like to acknowledge helpful discussions with Grisha Falkovich, Omri Golan, Leonid Levitov, Michal Shavit and Andrey Shytov. This research was enabled in part by support provided by Compute Canada (www.computecanada.ca).

SI acknowledges the Leona M. and Harry B. Helmsley Charitable Trust grant, ISF grant (1182/21) and the Minerva grant (713237). TS acknowledges the support of the Natural Sciences and Engineering Research Council of Canada (NSERC), in particular the Discovery Grant [RGPIN-2020-05842], the Accelerator Supplement [RGPAS-2020-00060], and the Discovery Launch Supplement [DGEER-2020-00222]. AS was supported by the ERC under the Horizon 2020 Research and Innovation programme (LEGOTOP No. 788715), the DFG (CRC/Transregio 183, EI 519/7-1), and the ISF Quantum Science and Technology (2074/19)

-
- [1] R. Landauer, Spatial variation of currents and fields due to localized scatterers in metallic conduction, *IBM Journal of Research and Development* **1**, 223 (1957).
 - [2] Y. V. Sharvin, A Possible Method for Studying Fermi Surfaces, *Soviet Journal of Experimental and Theoretical Physics* **21**, 655 (1965).
 - [3] S. Datta, *Electronic Transport in Mesoscopic Systems*, Cambridge Studies in Semiconductor Physics and Microelectronic Engineering (Cambridge University Press, 1995).
 - [4] Y. Imry, *Introduction to mesoscopic physics* (Oxford University Press on Demand, 2002).
 - [5] R. Gurzhi, Minimum of resistance in impurity-free conductors, *Sov. Phys. JETP* **44**, 771 (1963).
 - [6] R. Gurzhi, Hydrodynamic effects in solids at low temperature, *Physics-Uspekhi* **11**, 255 (1968).
 - [7] J. E. Black, Contribution of electron-electron normal scattering processes to the electrical resistivity of thin wires, *Phys. Rev. B* **21**, 3279 (1980).
 - [8] Z. Z. Yu, M. Haerle, J. W. Zwart, J. Bass, W. P. Pratt, and P. A. Schroeder, Negative temperature derivative of resistivity in thin potassium samples: The gurzhi effect?, *Phys. Rev. Lett.* **52**, 368 (1984).
 - [9] R. Gurzhi, A. Kalinenko, and A. Kopeliovich, Electron-electron collisions and a new hydrodynamic effect in two-dimensional electron gas, *Physical review letters* **74**, 3872 (1995).
 - [10] L. W. Molenkamp and M. J. M. de Jong, Electron-electron-scattering-induced size effects in a two-dimensional wire, *Phys. Rev. B* **49**, 5038 (1994).
 - [11] M. J. M. de Jong and L. W. Molenkamp, Hydrodynamic electron flow in high-mobility wires, *Phys. Rev. B* **51**, 13389 (1995).
 - [12] M. Dyakonov and M. Shur, Shallow water analogy for a ballistic field effect transistor: New mechanism of plasma wave generation by dc current, *Phys. Rev. Lett.* **71**, 2465 (1993).
 - [13] E. Chow, H. P. Wei, S. M. Girvin, and M. Shayegan, Phonon emission from a 2d electron gas: Evidence of transition to the hydrodynamic regime, *Phys. Rev. Lett.* **77**, 1143 (1996).
 - [14] B. Spivak and S. A. Kivelson, Transport in two dimensional electronic micro-emulsions, *Annals of Physics* **321**, 2071 (2006).
 - [15] A. V. Andreev, S. A. Kivelson, and B. Spivak, Hydrodynamic description of transport in strongly correlated

- electron systems, *Phys. Rev. Lett.* **106**, 256804 (2011).
- [16] I. Torre, A. Tomadin, A. K. Geim, and M. Polini, Non-local transport and the hydrodynamic shear viscosity in graphene, *Phys. Rev. B* **92**, 165433 (2015).
- [17] P. S. Alekseev, Negative magnetoresistance in viscous flow of two-dimensional electrons, *Phys. Rev. Lett.* **117**, 166601 (2016).
- [18] A. Tomadin, G. Vignale, and M. Polini, Corbino disk viscometer for 2d quantum electron liquids, *Phys. Rev. Lett.* **113**, 235901 (2014).
- [19] L. Levitov and G. Falkovich, Electron viscosity, current vortices and negative nonlocal resistance in graphene, *Nat Phys* **12**, 672 (2016).
- [20] A. Principi, G. Vignale, M. Carrega, and M. Polini, Bulk and shear viscosities of the two-dimensional electron liquid in a doped graphene sheet, *Phys. Rev. B* **93**, 125410 (2016).
- [21] M. Sherafati, A. Principi, and G. Vignale, Hall viscosity and electromagnetic response of electrons in graphene, *Phys. Rev. B* **94**, 125427 (2016).
- [22] H. Guo, E. Ilseven, G. Falkovich, and L. Levitov, Stokes Paradox, Back Reflections and Interaction-Enhanced Conduction, ArXiv e-prints (2016), [arXiv:1612.09239](https://arxiv.org/abs/1612.09239) [[cond-mat.mes-hall](https://arxiv.org/abs/1612.09239)].
- [23] A. Lucas, Stokes paradox in electronic fermi liquids, *Phys. Rev. B* **95**, 115425 (2017).
- [24] A. Levchenko, H.-Y. Xie, and A. V. Andreev, Viscous magnetoresistance of correlated electron liquids, *Phys. Rev. B* **95**, 121301 (2017).
- [25] D. A. Bandurin, I. Torre, R. K. Kumar, M. Ben Shalom, A. Tomadin, A. Principi, G. H. Auton, E. Khestanova, K. S. Novoselov, I. V. Grigorieva, L. A. Ponomarenko, A. K. Geim, and M. Polini, Negative local resistance caused by viscous electron backflow in graphene, *Science* **351**, 1055 (2016).
- [26] J. Crossno, J. K. Shi, K. Wang, X. Liu, A. Harzheim, A. Lucas, S. Sachdev, P. Kim, T. Taniguchi, K. Watanabe, T. A. Ohki, and K. C. Fong, Observation of the dirac fluid and the breakdown of the wiedemann-franz law in graphene, *Science* **351**, 1058 (2016).
- [27] P. J. W. Moll, P. Kushwaha, N. Nandi, B. Schmidt, and A. P. Mackenzie, Evidence for hydrodynamic electron flow in PdCoO_2 , *Science* **351**, 1061 (2016).
- [28] B. N. Narozhny, I. V. Gornyi, A. D. Mirlin, and J. Schmalian, Hydrodynamic approach to electronic transport in graphene, *Annalen der Physik* **529**, 1700043 (2017).
- [29] H. Guo, E. Ilseven, G. Falkovich, and L. S. Levitov, Higher-than-ballistic conduction of viscous electron flows, *Proceedings of the National Academy of Sciences* **114**, 3068 (2017).
- [30] R. Krishna Kumar, D. A. Bandurin, F. M. D. Pellegrino, Y. Cao, A. Principi, H. Guo, G. H. Auton, M. Ben Shalom, L. A. Ponomarenko, G. Falkovich, K. Watanabe, T. Taniguchi, I. V. Grigorieva, L. S. Levitov, M. Polini, and A. K. Geim, Superballistic flow of viscous electron fluid through graphene constrictions, *Nature Physics* **13**, 1182 (2017).
- [31] A. Lucas and S. A. Hartnoll, Kinetic theory of transport for inhomogeneous electron fluids, *Phys. Rev. B* **97**, 045105 (2018).
- [32] D. Y. H. Ho, I. Yudhistira, N. Chakraborty, and S. Adam, Theoretical determination of hydrodynamic window in monolayer and bilayer graphene from scattering rates, *Phys. Rev. B* **97**, 121404 (2018).
- [33] A. Shytov, J. F. Kong, G. Falkovich, and L. Levitov, Particle collisions and negative nonlocal response of ballistic electrons, *Phys. Rev. Lett.* **121**, 176805 (2018).
- [34] P. S. Alekseev and M. A. Semina, Ballistic flow of two-dimensional interacting electrons, *Phys. Rev. B* **98**, 165412 (2018).
- [35] D. Svintsov, Hydrodynamic-to-ballistic crossover in dirac materials, *Phys. Rev. B* **97**, 121405 (2018).
- [36] J. Gooth, F. Menges, N. Kumar, V. Süß, C. Shekhar, Y. Sun, U. Drechsler, R. Zierold, C. Felser, and B. Gotsmann, Thermal and electrical signatures of a hydrodynamic electron fluid in tungsten diphosphide, *Nature Communications* **9**, 4093 (2018).
- [37] B. A. Braem, F. M. D. Pellegrino, A. Principi, M. Rössli, C. Gold, S. Hennel, J. V. Koski, M. Berl, W. Dietsche, W. Wegscheider, M. Polini, T. Ihn, and K. Ensslin, Scanning gate microscopy in a viscous electron fluid, *Phys. Rev. B* **98**, 241304 (2018).
- [38] A. I. Berdyugin, S. G. Xu, F. M. D. Pellegrino, R. Krishna Kumar, A. Principi, I. Torre, M. Ben Shalom, T. Taniguchi, K. Watanabe, I. V. Grigorieva, M. Polini, A. K. Geim, and D. A. Bandurin, Measuring Hall viscosity of graphene's electron fluid, *Science* **364**, 162 (2019), [arXiv:1806.01606](https://arxiv.org/abs/1806.01606) [[cond-mat.mes-hall](https://arxiv.org/abs/1806.01606)].
- [39] J. A. Sulpizio, L. Ella, A. Rozen, J. Birkbeck, D. J. Perello, D. Dutta, M. Ben-Shalom, T. Taniguchi, K. Watanabe, T. Holder, R. Queiroz, A. Principi, A. Stern, T. Scaffidi, A. K. Geim, and S. Ilani, Visualizing poiseuille flow of hydrodynamic electrons, *Nature* **576**, 75 (2019).
- [40] M. Shavit, A. Shytov, and G. Falkovich, Freely flowing currents and electric field expulsion in viscous electronics, *Phys. Rev. Lett.* **123**, 026801 (2019).
- [41] M. J. H. Ku, T. X. Zhou, Q. Li, Y. J. Shin, J. K. Shi, C. Burch, L. E. Anderson, A. T. Pierce, Y. Xie, A. Hamo, U. Vool, H. Zhang, F. Casola, T. Taniguchi, K. Watanabe, M. M. Fogler, P. Kim, A. Yacoby, and R. L. Walsworth, Imaging viscous flow of the dirac fluid in graphene, *Nature* **583**, 537 (2020).
- [42] A. Levchenko and J. Schmalian, Transport properties of strongly coupled electron-phonon liquids, *Annals of Physics* **419**, 168218 (2020).
- [43] T. Holder, R. Queiroz, T. Scaffidi, N. Silberstein, A. Rozen, J. A. Sulpizio, L. Ella, S. Ilani, and A. Stern, Ballistic and hydrodynamic magnetotransport in narrow channels, *Phys. Rev. B* **100**, 245305 (2019).
- [44] A. Jenkins, S. Baumann, H. Zhou, S. A. Meynell, D. Yang, K. Watanabe, T. Taniguchi, A. Lucas, A. F. Young, and A. C. Bleszynski Jayich, Imaging the breakdown of ohmic transport in graphene, arXiv e-prints, [arXiv:2002.05065](https://arxiv.org/abs/2002.05065) (2020), [arXiv:2002.05065](https://arxiv.org/abs/2002.05065) [[cond-mat.mes-hall](https://arxiv.org/abs/2002.05065)].
- [45] A. C. Keser, D. Q. Wang, O. Klochan, D. Y. H. Ho, O. A. Tkachenko, V. A. Tkachenko, D. Culcer, S. Adam, I. Farrer, D. A. Ritchie, O. P. Sushkov, and A. R. Hamilton, Geometric control of universal hydrodynamic flow in a two-dimensional electron fluid, *Phys. Rev. X* **11**, 031030 (2021).
- [46] A. Gupta, J. J. Heremans, G. Kataria, M. Chandra, S. Fallahi, G. C. Gardner, and M. J. Manfra, Hydrodynamic and ballistic transport over large length scales in GaAs/AlGaAs, *Phys. Rev. Lett.* **126**, 076803 (2021).
- [47] Z. J. Krebs, W. A. Behn, S. Li, K. J. Smith, K. Watan-

- abe, T. Taniguchi, A. Levchenko, and V. W. Brar, Imaging the breaking of electrostatic dams in graphene for ballistic and viscous fluids, arXiv e-prints , arXiv:2106.07212 (2021), [arXiv:2106.07212 \[cond-mat.mes-hall\]](#).
- [48] Q. Hong, M. Davydova, P. J. Ledwith, and L. Levitov, Superscreening by a Retroreflected Hole Backflow in Tomographic Electron Fluids, arXiv e-prints , arXiv:2012.03840 (2020), [arXiv:2012.03840 \[cond-mat.mes-hall\]](#).
- [49] J. Callaway, Model for lattice thermal conductivity at low temperatures, *Phys. Rev.* **113**, 1046 (1959).

Supplemental material to “*Spread and erase - How electron hydrodynamics can eliminate the Landauer-Sharvin resistance*”

In this supplemental material, we give (A) the derivation of the Boltzmann equation in the wormhole geometry, (B) the solution of the Boltzmann equation in the hydrodynamic regime for a wormhole, (C) the solution of the Boltzmann equation in the hydrodynamic regime for a bar with a density variation, and (D) a discussion of the contact resistance.

Appendix A: Derivation of Boltzmann equation for the wormhole

The wormhole is a surface of revolution defined by $r(z)$ with coordinates $(r(z) \cos(\phi), r(z) \sin(\phi), z)$. The kinetic energy of a particle (which is also the Lagrangian) is given by

$$|v_F|^2 = (r\dot{\phi})^2 + \dot{z}^2(1 + r'^2) \quad (\text{A1})$$

and is conserved. Since the norm of the velocity is conserved, we only need to keep track of its angle θ :

$$\begin{aligned} r\dot{\phi} &= v_F \sin(\theta) \\ \sqrt{1 + r'^2}\dot{z} &= v_F \cos(\theta) \end{aligned} \quad (\text{A2})$$

The equations of motion are given by:

$$\begin{aligned} \ddot{\phi} &= -2\frac{r'}{r}\dot{z}\dot{\phi} \\ \ddot{z} &= \frac{rr'}{1 + r'^2}\dot{\phi}^2 - \frac{r'r''}{1 + r'^2}\dot{z}^2 \end{aligned} \quad (\text{A3})$$

Starting from the initial 2D problem with 2 coordinates and 2 velocities, we can get rid of ϕ by rotational symmetry, and we can only keep the angle θ to define the velocity since the norm of the velocity is conserved. In the end, we have a two-dimensional problem (r, θ) given by:

$$\begin{aligned} \dot{r} &= r'\dot{z} = \frac{r'}{\sqrt{1 + r'^2}}v_F \cos(\theta) \\ \dot{\theta} &= -\frac{r'}{r}\frac{1}{\sqrt{1 + r'^2}}v_F \sin(\theta) \end{aligned} \quad (\text{A4})$$

We can now write the Boltzmann equation for $f(r, \theta)$ as:

$$\frac{df}{dt} = \partial_r(f)\dot{r} + \partial_\theta(f)\dot{\theta} = v_F I[f] \quad (\text{A5})$$

with $I[f]$ the scattering integral given in the main text. This leads to

$$\partial_r(f)\frac{r'}{\sqrt{1 + r'^2}}\cos(\theta) - \partial_\theta(f)\frac{r'}{r}\frac{1}{\sqrt{1 + r'^2}}\sin(\theta) = I[f] \quad (\text{A6})$$

This can be rewritten as

$$\partial_r(f)\cos(\theta) - \partial_\theta(f)\frac{1}{r}\sin(\theta) = \frac{\sqrt{1 + r'^2}}{r'}I[f] \quad (\text{A7})$$

The left hand side is independent of z , which means in the ballistic regime, all surfaces are equivalent once expressed in terms of r . In the non-ballistic case, the only difference between surfaces is that the scattering rate acquires a dependence on r' through the factor $\sqrt{1 + r'^2}/r'$.

Appendix B: Wormhole and Corbino disk - solution of the Boltzmann equation in the hydrodynamic regime

The equation describing the non-equilibrium current distribution is obtained from Eq. (A7) by setting $f(\mathbf{p}, z) = \delta(\epsilon_F - \epsilon(\mathbf{p}))h^y(p_y)$ and integrating $p_F \int \frac{dp_x}{2\pi}$. We get,

$$\pm \left[\nu_F \partial_z h^y_{R,L} - \nu_F \frac{r'}{r} p_y \partial_{p_y} h^y_{R,L} \right] = \sqrt{1 + r'^2} \tilde{I}[h^y] \quad (\text{B1})$$

with,

$$\tilde{I}[h^y_{R,L}(\mathbf{p}, \mathbf{r})] = -\frac{\nu^y}{\ell_{ee}} \left[h^y_{R,L} - \frac{\rho(\mathbf{r})}{2\nu_F} \mp \frac{4\pi j_x(\mathbf{r})}{k_F} \sqrt{1 - (p_y/k_F)^2} \right] \quad (\text{B2})$$

The transformation of this equation to an equation for h^j is explained below. In this section we work with h^y .

1. Solving the Boltzmann equation to linear order in ℓ_{ee}

In this subsection we solve the equation for h^y up to first order in $\ell_{ee}r'/r$. For brevity, we define $k_y \equiv p_y/k_F$. The solution for h^j is obtained by setting $k_y = j/k_F r$ in the solution $h^y(k_y)$. We derive the Boltzmann equation directly for h^j in the next subsection, for completeness.

Assuming that $r(z)$ varies slowly on a scale of ℓ_{ee} we try as a first attempt the z -independent solution of a uniform r , adjusted at each point to the local $r(z)$, i.e., $h^y_{R,L}(k_y) = \pm \frac{2I}{k_F r(z)} \sqrt{1 - k_y^2}$. This attempted solution conserves current. Substituting it into Eq. (B1) we find on the l.h.s. a remainder term $-\frac{2I r'}{k_F r^2} \frac{1 - 2k_y^2}{\sqrt{1 - k_y^2}}$. It is linear in r' , as expected. To compensate for this term, we modify our solution, making it

$$\begin{aligned} h_{R,L}(k_y) &= \pm \frac{2I}{k_F r(z)} \sqrt{1 - k_y^2} + \frac{2I \ell_{ee} r'}{k_F r^2(z) \sqrt{1 + r'^2}} (1 - 2k_y^2) \\ &= \pm \frac{2I}{k_F r(z)} \sqrt{1 - k_y^2} + \frac{2I \ell_{ee} \sin \xi}{k_F r^2(z)} (1 - 2k_y^2) \end{aligned} \quad (\text{B3})$$

The term we added to h is linear in ℓ_{ee} , such that when substituted into the r.h.s, it balances the remainder term on the l.h.s., which is ℓ_{ee} -independent. However, it generates a new remainder term on the l.h.s., which is linear in ℓ_{ee} . Specifically, this term is,

$$\pm \left(\frac{2I \ell_{ee}}{k_F r^2} \xi' \cos \xi (1 - 2k_y^2) + \frac{4I r' \ell_{ee}}{k_F r^3} \sin \xi (4k_y^2 - 1) \right) \quad (\text{B4})$$

Naively, we should balance this term by adding a term $\delta h \propto \ell_{ee}^2$ to our solution, thereby generating a term $\delta h \nu^y / \ell_{ee}$ on the r.h.s to cancel the contribution (B4) on the l.h.s. We should note, however, that the r.h.s. cannot cancel parts of δh that carry a current or a density. Furthermore, we cannot add to h a term that carries current, because we assume a fixed driven current. As it turns out, the second term in (B4) can be cancelled by the r.h.s., but the first term requires more care. We write it as

$$\pm \left(\frac{I \ell_{ee}}{k_F r^2} \xi' \cos \xi + \frac{I \ell_{ee}}{k_F r^2} \xi' \cos \xi (1 - 4k_y^2) \right) \quad (\text{B5})$$

and cancel the first, k_y -independent, term by subtracting a k_y -independent, density carrying, term,

$$\int dz' \frac{I \ell_{ee}}{k_F r^2} \xi' \cos \xi \quad (\text{B6})$$

When divided by ν_F , this term gives the local electrochemical potential.

2. Deriving the Boltzmann equation for h^j

To get the Boltzmann equation that appears in (4), we start from Eq. (B1) and change the variables $z, p_y \rightarrow z, j$. Since $j = p_y r(z)$ we must treat the dependence between the coordinates carefully. It is easy to confirm that the second

term in the LHS of (B1) becomes $-j \frac{r'}{r} \partial_j h_{R,L}$, however, the first term also changes because it is a total derivative, $\partial_z h_{R,L} \rightarrow \partial_z h_{R,L} + \frac{\partial j}{\partial z} \partial_j h_{R,L}$. Using $\frac{\partial j}{\partial z} = p_y r'$ we get that

$$\frac{\partial j}{\partial z} \partial_j h_{R,L} - j \frac{r'}{r} \partial_j h_{R,L} = 0,$$

thus obtaining Eq. (4).

Appendix C: Bar with a density variation - solution of the Boltzmann equation for the hydrodynamic regime

We consider an infinite bar parallel to the z -axis, in which the equilibrium density, and hence k_F vary with z . Furthermore, with a variation of density comes also a variation of ℓ_{ee} . When the walls of the bar are specular, we can view it as a cylinder, and we denote the circumference by $2\pi r$. With these assumptions, Boltzmann equation (4) and the collision term (8) remain the same as they were for a wormhole, with $r' = 0$:

$$\pm \frac{\nu_F}{\nu_j} \partial_z h_{R,L} = -\frac{1}{\ell_{ee}} \left[h_{R,L} - \frac{\rho}{2\nu_F} \mp \frac{4\pi j_x}{k_F} \sqrt{1 - \left(\frac{j}{k_F r}\right)^2} \right] \quad (\text{C1})$$

For the limit of small ℓ_{ee} , we first try as a naive ℓ_{ee} -independent solution the locally Galilean boosted Fermi sphere: $h_{R,L} = \pm \frac{2I}{k_F r} \sqrt{1 - \left(\frac{j}{k_F r}\right)^2}$, and we aim to find all corrections of order ℓ_{ee} to this term. Any amendment we do to the naive solution should not carry current, since the current is fixed to I . When the naive solution is substituted in (C1) the right hand side vanishes since $I = 2\pi r j_x$ and $\rho = 0$. However we get an extra term of $-\frac{2Ik'_F}{k_F^2 r} \left(1 - 2\left(\frac{j}{k_F r}\right)^2\right)$ on the LHS. We can balance this term by adding to our solution $\frac{2I\ell_{ee}k'_F}{k_F^2 r} \left(1 - 2\left(\frac{j}{k_F r}\right)^2\right)$.

This amended solution solves (C1), up to a remainder term on the LHS:

$$\sqrt{1 - \left(\frac{j}{k_F r}\right)^2} \partial_z \left[\frac{2I\ell_{ee}k'_F}{k_F^2 r} \left(1 - 2\left(\frac{j}{k_F r}\right)^2\right) \right] \quad (\text{C2})$$

This remainder term is of the order ℓ_{ee} and we need to amend our solution further to eliminate it. In principle, there are two ways to do that. The part of (C2) that does not carry density or current can be eliminated by an addition of a term of order ℓ_{ee}^2 to h . Such a term will yield an order ℓ_{ee} term on the RHS. However, being a contribution to h that is of order ℓ_{ee}^2 , it is beyond our scope. The part of (C2) that carries density of current, on the other hand, should be canceled by adding a term of order ℓ_{ee} to h , that is purely a density term. Such a term will not affect the RHS, and its substitution in the LHS will cancel the terms in (C2). It is this term we are after. An inspection of (C1) and (C2) allows us to find it and write the full expression of h to linear order in ℓ_{ee} as

$$\begin{aligned} h_{R,L}^j &= \pm \frac{2I}{k_F r} \sqrt{1 - \left(\frac{j}{k_F r}\right)^2} \\ &+ \frac{2I\ell_{ee}}{k_F^2 r} k'_F \left(1 - 2\left(\frac{j}{k_F r}\right)^2\right) \\ &- I \int^z d\tilde{z} \frac{(k'_F \ell_{ee})'}{2k_F^2 r} \end{aligned} \quad (\text{C3})$$

where in the integrand in the last term k_F, ℓ_{ee} are both functions of \tilde{z} .

Appendix D: Contact resistance

At the contact the density variation is fast. As a consequence the full solution of the Boltzmann equation becomes hard to obtain, but we can still estimate the voltage drop on the contact region. For the simplest case of a ballistic cylinder ($\xi = 0$), or a ballistic rectangular-shaped conductor with specular walls, the entire potential drop is on the

two contacts. By symmetry, at the center of the wormhole $h_R^j = -h_L^j = \frac{I}{2k_F r}$ and consequently $V = 0$. In fact, these values of h_R^j, h_L^j hold anywhere within the sample, at $|z| < L/2$. In the contacts ($z = \pm(L/2 + \epsilon)$) themselves $h_R^j = h_L^j$, and their value is determined by the local potential. Thus, there is a jump in the value of h_L^j at $z = -L/2$ and of h_R^j at $z = L/2$, and this jump leads to the expected jump of the potentials at the contacts.

Next, we think of the cylindrical geometry with electron-electron scattering. Far from the contacts (a distance much larger than ℓ_{ee}) our main-text analysis holds, leading to $h_R^j = -h_L^j = \frac{4\pi J_x}{k_F} \sqrt{1 - (j/k_F r)^2}$ and $V = 0$. At the two contacts $h_R^j = h_L^j = \pm V(I)/2$, and it is $V(I)$ that we estimate now. For clarity we focus on the left contact, at $z = -L/2$.

The equations satisfied by $h_{R,L}^j$ are of the form

$$\pm \nu_F \partial_z h_{R,L}^j(j, z) = -\frac{\nu^j}{\ell_{ee}} \left[h_{R,L}^j - \frac{\rho(z)}{\nu_F} \mp \frac{4\pi J_x}{k_F} \sqrt{1 - \left(\frac{j}{k_F r}\right)^2} \right] \quad (\text{D1})$$

These equations are equivalent to,

$$h_{R,L}^j = h_{R,L}^j(\pm L/2) e^{\frac{\pm(z \pm L/2)\nu_j}{\nu_F \ell_{ee}}} + \int_{z_i}^z dz' \frac{\nu_j}{\nu_F \ell_{ee}} \left[-\frac{\rho(z')}{\nu_F} \mp \frac{4\pi J_x}{k_F} \right] e^{\frac{\pm(z \pm z')\nu_j}{\nu_F \ell_{ee}}} \quad (\text{D2})$$

Here, $h_{R,L}^j(\pm L/2)$ are the boundary conditions for the right- and left- moving electrons at the points where they enter the sample. The dependence of the distribution functions $h_{R,L}^j$ on z near the left contact is very different for the left- and right- moving electrons. For the left-moving electrons the entry point is very far from the contact we look at, and therefore the initial condition is long forgotten. In the bulk, the distribution of the left moving electrons does not vary in space, and since the second term in Eq. (D2) averages over a scale of ℓ_{ee} , we expect the variation of h_L^j to be slow even close to the contact.

For the right-moving electrons, in contrast, near the contact the solution is dominated by initial conditions. The distribution function, that starts as a constant $h_R^j = \pi^2 J_x / k_F$, decays into $h_R^j = \frac{4\pi J_x}{k_F} \sqrt{1 - (j/k_F r)^2}$, at a distance ℓ_{ee}/ν_j from the contact.

Motivated by these considerations, we make the ansatz,

$$\begin{aligned} h_L^j &\approx -\frac{4\pi J_x}{k_F} \sqrt{1 - (j/k_F r)^2} \\ h_R^j &= \frac{\pi^2 J_x}{k_F} e^{-(z+L/2)\nu^j/\nu_F \ell_{ee}} + (1 - e^{-(z+L/2)\nu^j/\ell_{ee}\nu_F}) \frac{4\pi J_x}{k_F} \sqrt{1 - (j/k_F r)^2} \end{aligned} \quad (\text{D3})$$

Within this ansatz, the voltage difference between the contact itself and the bulk is the same as it is in the ballistic case, namely half of the Landauer-Sharvin voltage drop falls on each contact. The effect of the scattering term is limited to distributing this voltage drop from being at the interface itself to being spread on a scale of ℓ_{ee} .